Journal of Applied Sciences

ISSN 1812-5654

Journal of Applied Sciences 9 (1): 197-200, 2009
ISSN 1812-5654

Electrical Investigations of $YBa_2Cu_3O_{(7-x)}$ ($0 \le x \le 0.5$) Tunnel Junctions

B. Chouial and B. Hadjoudja
Laboratory of Semiconductors, Department of Physics, University Badji Mokhtar, Annaba, Algeria

Abstract: In this study, we investigate superconducting tunnelling junctions based on high T_c $YBa_2Cu_3O_{(7-x)}$ ($0 \le x \le 0.5$) superconductors. Prepared junctions were characterised at different temperatures and several voltage ranges. It was found that the measured current-voltage as well as conductance characteristics exhibited good superconducting behaviour. Many properties such as the zero voltage anomaly and gap anisotropy were put into evidence.

Key words: $YBa_2Cu_3O_{(7-x)}$, superconductor, tunnel junctions, conductance, gap parameter

INTRODUCTION

Since the discovery of High Temperature Superconductor (HTS), a world wide intense research has been triggered among the scientific community. This has led to the discovery of many HTS whose T_c is well above the boiling point of liquid nitrogen and thus had considerable consequences on both scientific and commercial instrumentation using devices based on high T_c superconducting materials such as $YBa_2Cu_3O_{(7-x)}$ ($0 \le x \le 0.5$) or YBCO in short with a $T_c = 90$ K. Its structure is orthorhombic and has two main features: the planes parallel to (a, b) which are referred to as planes layers and those parallel to c and referred to a chains. These plane layers and chains have different properties like the resistivity ρ and the energy gap Δ. The oxygen content is critical as it has direct implications on the properties of YBCO: the quality of the superconducting material increases with the oxygen within the lattice. Thus, oxygen is a key element. Other materials have been found to have different effects on YBCO such as the effect of the substrates and the doping on T_c (Spankova *et al*., 2002) and Δ (Thomsen *et al*., 1991). Other parameters which characterise the superconductors such as the coherence length ξ_0, the penetration depth λ, the critical current J_c and the critical magnetic field H_c are related to T_c and Δ. Each of these parameters can prove to be crucial for different applications. Therefore, particular attention must be given to the doping levels during sample preparation. The device at the heart of many superconductor device applications is the superconductor tunnel junction. The most common is the planar oxide tunnel junction (junction with artificial barrier) (Plecenik *et al*., 2000). There exist several other types of junctions or weak link as they are referred to because the critical current J_c in the active area of the device is lower than the current in the superconductor on either side of the junction. The most widely used weak links are the thin film bridge junction and the point contact junction. High T_c superconductors are characterized by the so called native junctions or weak links which are due to the granular nature of these materials. Many devices such as detectors (Kislinskii *et al*., 2002), mixers (Xu *et al*., 2007), SQUIDS (Charlebois *et al*., 2004; Bauch *et al*., 2007), resonators (Seron *et al*., 2006) and bolometers (Delerue *et al*., 2003) have been built on YBCO superconductor. This study report on the electrical characterization of junctions built on YBCO.

MATERIALS AND METHODS

Sample preparation: The sample was cut from a superconducting pellet. Aluminium was deposited on it and heated for 10 min in an oven at 100°C, on the half-upper side of the sample, to yield Al_2O_3. Silver dots were then evaporated to form the normal metal electrodes of the junctions. The back contact was ensured by the whole Ag-covered bottom side of the sample.

Experimental set up: The sample was mounted on the sample holder of a low temperature cryostat and connected to a computer controlled measurement set up which is shown in Fig. 1. This experimental set up consists of a programmable dc voltage source which generates the required voltage, V_g, into a circuit containing a box of resistances, R_s, in series with the junction. In parallel with the sample is a Thurlby intelligent multimeter which is used to measure the voltage across the connected junction, V_j.

Corresponding Author: Baghdadi Chouial, Laboratory of Semiconductors, Department of Physics, University Badji Mokhtar, Annaba, Algeria Fax: 213-38-87-53-99

Experimental procedure: Several different ranges of temperature can be reached with this cryostat: the 80 K range is obtained by keeping the sample under vacuum and filling the outer jacket with liquid N_2. The system allows the temperature to be lowered to 54 K by introducing liquid N_2 into the sample compartment and pumping it out gradually. Lower temperatures down to 4.2 K can be reached by filling the sample compartment with liquid Helium. The sample dots were connected to electrical contacts.

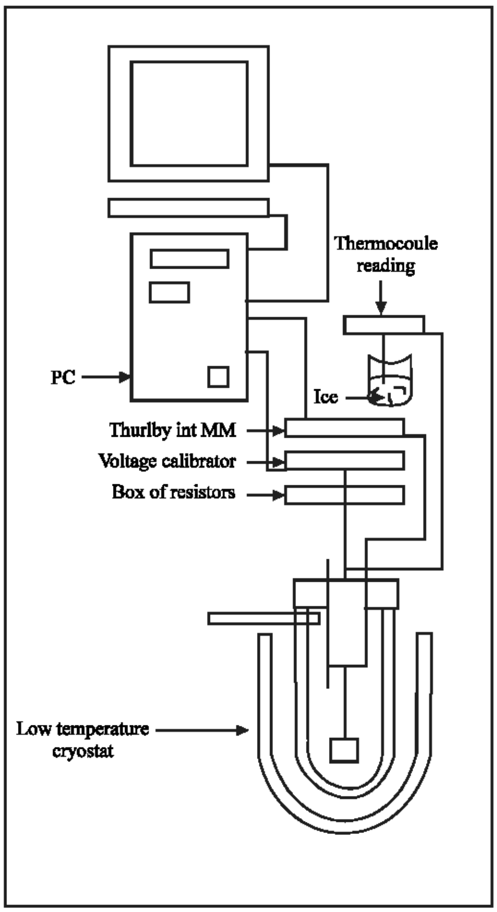

Fig. 1: Schematic diagram of the experimental set up

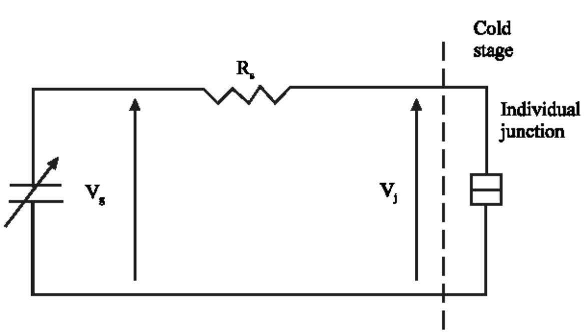

Fig. 2: Equivalent circuit of the experimental set up

The measurement system is represented by the circuit shown in Fig. 2. The voltage V_g was automatically varied over large range (from ±10 to ±300 mV). For each voltage the current flowing through the junction I_j is calculated by the same program using the formula:

$$I_j = (V_g - V_j)/R_s$$

The corresponding values of V_j and I_j obtained constitute the data which are stored in the computer and processed to yield the I = f(V) and dI/dV = f(V) characteristics.

RESULTS AND DISCUSSION

The I-V curve is characterized by a slight increase in current around 0 V and two strong non-linearities at ±35 mV and two small negative differential resistances, NDR, like features at ±65 mV (Fig. 3). The conductance plot shown in Fig. 4 highlights the features of Fig. 3. The major features are two symmetrical peaks at ±33 mV and a smaller peak at 0 V which is 22 mV wide. Two other peaks can be seen at -100 and +97 mV.

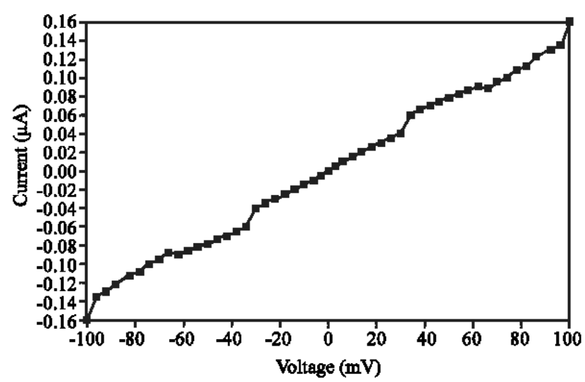

Fig. 3: IV curve of the first junction, T = 66 K, Rs = 500 Ω

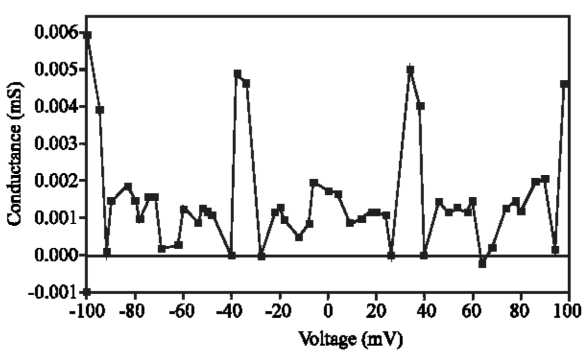

Fig. 4: Conductance versus voltage of the first junction, T = 66 K

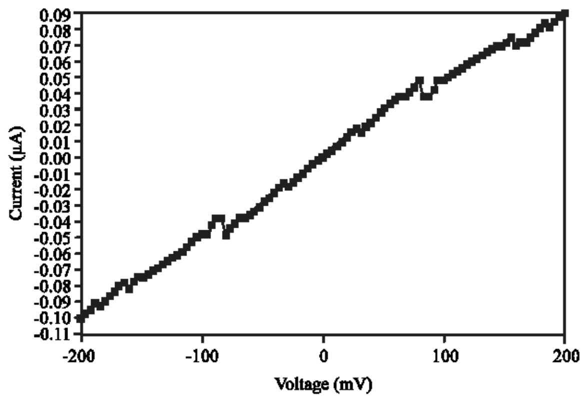

Fig. 5: I-V curve of the second junction, T = 54 K, R_s = 1000 Ω

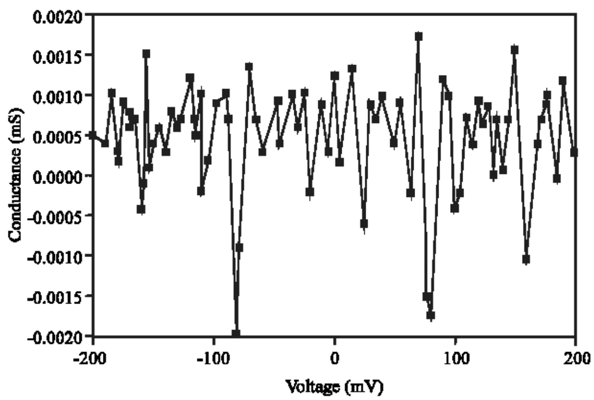

Fig. 6: Conductance versus voltage of the second junction, T = 54 K

Figure 5 shows the I-V curve of the second junction which exhibits very pronounced NDR-like features at ±83 mV. Additional but less pronounced features can be seen at ±19 and ±62 mV.

Figure 6 shows the conductance as a function of voltage obtained from the data of Fig. 5. This conductance curve has striking symmetrical features such as peaks at 0 V, ±41.5 and ±127.7 mV. The peaks at ±41.5 mV are enfolded by negative conductance resulting from very pronounced valleys at ±83 mV. These valleys possess some shoulder like features.

Figure 7 shows that at room temperature, all the low temperature features of the second junction including the NDR have vanished leaving a straight line.

The I-V curves of the investigated sample exhibit two types of non-linearities:

- I-V curves with pronounced non-linearities as is shown in Fig. 3. These features are reflected in the conductance versus voltage (Fig. 4) by peak features one at 0 V and two others at ±35 mV. The 0 V peak

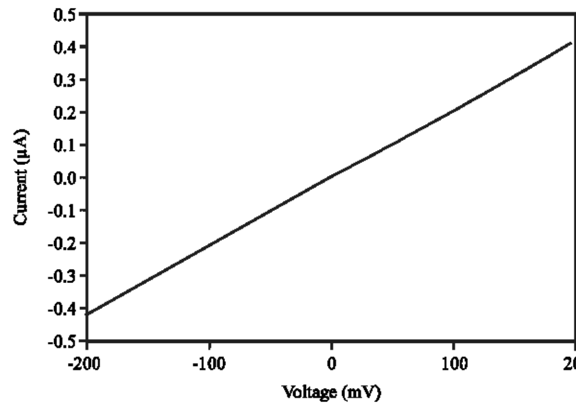

Fig. 7: I-V curve of the second junction, T = 296 K, R_s = 1000 Ω

has been reported in conductance versus voltage in junction having artificial barrier and was referred to as an anomaly. This peak has also been observed in point contact junctions and was explained in terms of superconducting weak link or Josephson-like current flowing through a non-ideal barrier. In the case of the peak features similar to that of Fig. 4, a method of energy gap determination was suggested (Igushi and Wen, 1991) in which the 0 V peak was interpreted to be due to an energy gap along the c axis, Δ_c and the two other peaks which enclose it, were identified with the energy gap in the (a, b) planes Δ_{ab}. The values suggested in this investigation are:

$$\Delta_c = 5 \text{ meV}$$
$$\Delta_{ab} = 16 \text{ to } 20 \text{ meV}$$

If this method is applied to the features of Fig. 4, one obtains the energy gap value of 11 meV in the c direction and 33 meV in the (a, b) planes. As the reported values of Δ_c fall in the range 3 to 6 meV (Igushi and Wen, 1991), this suggests the existence of an array of N junctions so that one can write:

For N junctions:	$N\Delta_c$	= 11 meV
	$N\Delta_{ab}$	= 33 meV
For N = 2:	Δ_c	= 5.5 meV
	Δ_{ab}	= 16.5 meV
For N = 3:	Δ_c	= 3.6 meV

The idea of array of networks of junction is widely used and results from the microstructure of the pellet which consists of a network of tiny grains which are randomly oriented. The coupling between the adjacent grains is weakened as a result of misalignments and contamination by impurity phases at the grain boundaries.

These grain boundaries act as week links and can be used in many applications such as detection, mixing and radiation emission.

- Curves with NDR features (Fig. 5). These features were reproducible over many scans. The conductance versus voltage curve (Fig. 6) gave a highly symmetrical structure of peaks including one at 0 V and valleys with one having negative value at ±83 mV. It is worth noting that NDR behaviour have been observed elsewhere (Luiz *et al*., 1997)

CONCLUSION

Superconducting tunnelling junctions based on high T_c $YBa_2Cu_3O_{(7-x)}$ $(0\leq x\leq 0.5)$ superconductors were experimentally investigated and highly non linear I-V were obtained in addition of their conductance. The gap parameters have been deduced from these curves and the obtained values are in agreement with those reported in the literature particularly when we consider the idea of array of networks of junction resulting from the weakened coupling between the adjacent grains because of misalignments and contamination by impurity phases at the grain boundaries.

REFERENCES

Bauch, T., J. Johansson, K. Cedergren, T. Lindström and F. Lombardi, 2007. YBCO SQUIDs with unconventional current phase relation. Physica. C: Supercond., 463: 979-984.

Charlebois, S.A., T. Lindström, A.Y. Tzalenchuk, Z. Ivanov and T. Claeson, 2004. Unconventional current-phase relation in YBCO DC SQUIDs. Physica. C: Supercond., 408: 926-927.

Delerue, J., A. Gauge, P. Teste, E. Caristan and G. Klisnick *et al*., 2003. YBCO mid-infrared bolometer arrays. IEEE Trans. Appl. Supercond., 13: 176-179.

Igushi, I. and Z. Wen, 1991. Tunnel gap structure and tunnelling model of the anisotropic YBaCuO/I/Pb junctions. Physica. C, 178: 1-10.

Kislinskii, Y.V., K.Y. Constantinian, I.V. Borisenko, G.A. Ovsyannikov and P. Yagoubov, 2002. Submilimeter wave signal detection by bycristal YBCO josphson junction at liquid nitrogen temperatures. Physica. C: Supercond., 372: 436-439.

Luiz, A.M., L.A.A. Pereira and R. Nicolsky, 1997. Heterodyne detector using a SNS junction. IEEE Trans. Applied Supercond., 7: 3719-3721.

Plecenik, A., V. Strbik, S. Chromik, M. Zuzcak and S. Benacka, 2000. Interface properties of $YBa_2Cu_3O_{7-x}$/I/metal junctions with native and artificial barriers. Supercond. Sci. Technol., 13: 1180-1185.

Seron, D., H. Kokabi, G. Alquie, Y. Roelens and N. Bourzgui *et al*., 2006. Characterization of microwave properties of YBCO superconducting coplanar resonators on different substrates deposited by thermal co-evaporation. J. Supercond., 1557: 1939-1947.

Spankova, M., I. Vavra, S. Chromik, S. Gazi and V. Strbik *et al*., 2002. Improvement of the superconducting properties of YBCO thin films upon annealing of C_eO_2/Al_2O_3 substrate. Thin Solid Films, 416: 254-259.

Thomsen, C., B. Friedl, M. Cieplak and M. Cardona, 1991. Effect of substitutional impurities on the superconducting gap of $YBa_2Cu_3O_{7-\delta}$. Solid State Commun., 78: 727-733.

Xu, W.W., Y.F. Zhang, X.K. Jiang, K. Ling and J. Chen *et al*., 2007. Performance improvements of a microwave oscillator using high temperature superconducting harmonic mixer. IEEE Trans. Applied Supercond., 17: 938-941.